LAWRENCE
LIVERMORE
NATIONAL
LABORATORY

LLNL-CONF-767544

An experimental and modeling study of autoignition for cyclopentane and dimethyl ether binary blends

S. W. Wagnon, N. Lokachari, G. Kukkadapu, H. J. Curran, W. J. Pitz

February 7, 2019

11th U. S. National Combustion Meeting
Pasadena, CA, United States
March 24, 2019 through March 27, 2019

Disclaimer

11th U. S. National Combustion Meeting
Organized by the Western States Section of the Combustion Institute
March 24–27, 2019
Pasadena, California

An experimental and modeling study of autoignition for cyclopentane and dimethyl ether binary blends

Scott W. Wagnon[1,], Nitin Lokachari[2], Goutham Kukkadapu[1], Henry J. Curran[2], William J. Pitz[1]*

[1]Lawrence Livermore National Laboratory, Livermore, CA 94551
[2]National University of Ireland, Galway, Ireland
[*]Corresponding Author Email: wagnon1@llnl.gov

Naphthenes (cycloalkanes) are often present in commercial transportation fuels at concentrations ranging from ~10-35% liquid volume. In gasoline, the most abundant naphthenes contain ~5-7 carbon atoms, making cyclopentane the smallest practical naphthenic surrogate compound for use in surrogate mixtures to represent gasoline. Neat cyclopentane is relatively unreactive, with a research octane number of 103 and an octane sensitivity of 18, properties that make it attractive as a blending component for gasoline. It is important to have experimental data to validate kinetic models for cyclopentane's autoignition behavior in mixtures if it is to be used as a component in surrogate mixtures representing gasoline. However, its low reactivity can challenge efforts to characterize it in fundamental facilities such as shock tubes and rapid compression machines. While recent studies by Al Rashidi et al. have focused on neat cyclopentane, there is little data available regarding how cyclopentane behaves in mixtures. Therefore, this study addresses both issues by using the NUI Galway experimental facilities to study binary mixtures of cyclopentane (CPT) and dimethyl ether (DME), a small well-characterized reactive compound. In this study, ignition delay times were measured for two binary mixtures, 30:70-CPT:DME and 70:30-CPT:DME (molar), at elevated pressures (20, 40 bar), several equivalence ratios (0.5, 1.0, 2.0), and across temperatures from 650-1350K. A revised detailed kinetic model for cyclopentane was also developed with additional validations from literature jet-stirred reactor and laminar flame speed measurements. The current work highlights the importance of resonantly stabilized radicals such as allyl, cyclopentenyl, and cyclopentadienyl in the combustion chemistry of cyclopentane.

Keywords: gasoline surrogates; shock tube; rapid compression machine; detailed chemical kinetic model

1. Introduction

Cyclopentane is a curious compound due to its high octane sensitivity (RON-MON = 18) measured in engine experiments despite exhibiting strong non-Arrhenius behavior as observed in several fundamental experiments [1,2,3]. Cyclopentane is also of interest because it represents the smallest practical surrogate compound of naphthenes for commercial transportation fuels. For these reasons, recent studies have sought to better understand the combustion chemistry of cyclopentane [4,5,6,7,8,9,10]. Other naphthenes considered for a fuel surrogate palette often include methyl cyclopentane, cyclohexane, and methyl cyclohexane and their studies have provided additional valuable insights into naphthenes [3,11,12].

Based on the existing literature studies of cyclopentane two related opportunities for new insights motivated the current work. The first opportunity stems from the relatively slow ignition delay times of neat cyclopentane at low temperatures. Slow ignition delay times can represent a challenge to measure in shock tubes and potentially complex physics to model in rapid compression machines. More practical ignition delay times can be measured using a second more reactive compound as a reactivity enhancer. Using a second compound in a binary blend with

cyclopentane presents an additional opportunity, as binary or more complex mixtures with cyclopentane have not been extensively studied. In this study, dimethyl ether (DME) was selected as a blending agent for being significantly more reactive than cyclopentane (CPT), and for being the compound with the simplest chemistry that exhibits behaviors of negative temperature coefficient (NTC) and two-stage ignition [13,14].

2. Experimental methods

All ignition delay time (IDT) measurements in this study were performed in the high pressure shock tube (HPST) and rapid compression machine (RCM) facilities at NUI Galway. Relatively short ignition delay times (0.02~7 ms) were measured in the HPST while longer IDTs (4~350 ms) were measured in the RCM. The total ignition delay time was determined using the time of maximum rate of pressure rise in the devices. The uncertainty in the IDT's were ±10% in the HPST and ±15% in the RCM. These facilities complement each other by permitting the measurement of a wide range of IDTs as a function of temperature. The experiments performed in these two facilities are listed in Table 1. For the experiments, test fuels (dimethyl ether-99.5% and cyclopentane-99%) were supplied by Sigma Aldrich. The other gases used in this study, nitrogen (99.99%), oxygen (99.99%) and helium (99.97%) were purchased from BOC Ireland and used without further purification. Fuel-air mixtures were prepared in an external stainless-steel vessel by employing partial pressure method and allowed to diffusively mix for at least 12 h before the experiments. A brief description of the HPST and RCM are provided here.

2.1 Rapid compression machine (RCM)

The RCM at NUIG has an opposed twin piston arrangement with 38 mm bore and 168 mm stroke. The pre-mixed fuel/air mixture is introduced into the reaction chamber and is rapidly compressed in ~16 ms by the pistons. Creviced piston heads were used to largely limit the turbulence/ roll-up vortices generated in the test gas [15]. The pistons are pneumatically driven and locked at the end of compression, creating a constant volume condition. After the end of compression, the pressure drops due to the heat loss from the gas mixture to the reaction chamber walls. The RCM is equipped with a piezoelectric pressure sensor (Kistler 6045A) on the side wall of the reaction chamber to enable time-resolved pressure measurements of the test mixture.

Pyrolytic, or so-called non-reactive, experiments were conducted by replacing oxygen in the test mixture with N_2 to create effective volume histories as input for simulations to capture compression and heat transfer effects. The initial temperature of the RCM system is adjusted to attain different compressed temperatures of the test mixture. Experimental compressed temperatures were calculated assuming isentropic conditions in 'Gaseq' [16].

2.2 High pressure shock tube (HPST)

High temperature IDTs of the binary blends were measured behind the reflected shock waves. The HPST with uniform cross-section area of 63.5 mm inner diameter consists of a 3 m long driver section to hold high pressure and low molecular weight gas (helium), 5.7 m long driven section that contains the heavier test gas. A 30 mm double diaphragm section with pre-scored aluminum discs of appropriate thickness, separates the driver and driven sections and enables improved control over the shock waves generated.

The shock wave travels through the driven section and rapidly compresses and heats the test gas to a desired thermodynamic condition at the end-wall before it ignites. By varying the Mach number of the shock wave, the final compressed conditions of the test gas are also varied. Parts of helium driver gas is replaced with a heavier inert gas (nitrogen) to delay the arrival of the contact surface at the end-wall and to increase the measuring times (≥ 1.5 ms). Six PCB 113B24 piezoelectric pressure transducers are mounted on the side wall of the driven section and one

Kistler 603B sensor on the end-wall are used to extrapolate the shock velocity calculation at the end-wall. The Kistler sensor is also used to record pressure profiles that are used to record/measure the IDTs. The measured shock velocity is used to calculate the compressed pressure and temperature using the 'reflected shock' routine in Gaseq [16].

Table 1. Nominal conditions and binary mixture compositions of this study

CPT:DME [molar ratio]	φ	O_2 [molar]	N_2 [molar]	p [bar]	T [K]	Facility
30:70	0.5, 1.0, 2.0	21%	79%	20, 40	650–1350	HPST, RCM
70:30	0.5, 1.0, 2.0	21%	79%	20, 40	650–1350	HPST, RCM

3. Development of the detailed kinetic model

The current chemical kinetic model for cyclopentane was developed from the basis of a small hydrocarbon (C0~C4) kinetic model from NUIG [17] and previous kinetic modeling of cyclopentane by Al Rashidi et al. [4]. Aromatic chemistry stemming from cyclopentadiene and cyclopentadienyl pathways was required and sub-models from the study by Kukkadapu et al. [18] were included. The resulting merged model was unsatisfactory in performance when validated against the current measurements and literature data. Therefore, a critical re-evaluation of the cyclopentane, cyclopentene, cyclopentadiene and dimethyl ether sub-models was undertaken and will be discussed in the following sections. Additional comments and citations can be found next to each relevant reaction in the kinetics file for those not explicitly discussed in the main text.

The thermochemistry species data were taken from the references above. If new thermochemistry was needed for a species, Benson's group additivity methods as implemented in THERM [19] were applied to estimate properties (i.e. enthalpy, entropy, heat capacity). Transport properties for the small hydrocarbon species were included from the NUIG model [17], and new transport properties for larger species unavailable from previous work were estimated using the methods of Dooley et al. [20] and Bosque and Sales [21]. Simulations for ignition delay times utilized the Lawrence Livermore National Laboratory (LLNL) developed software ZeroRK [22], including non-reactive volume histories for the RCM experiments and a constant volume for ST experiments. Additional literature experiments (e.g. jet-stirred reactor, flame speeds) were simulated using the appropriate CHEMKIN-Pro [23] modules as necessary.

3.1 Cyclopentane sub-model

Unimolecular decomposition via the carbon-carbon bonds in cyclopentane has long been thought to proceed primarily via formation of a diradical and prompt H-atom transfer forming 1-pentene [24,25]. An alternative unimolecular decomposition involving the carbon-carbon bonds includes the formation of ethylene and cyclopropane [24,25]. In the current study, the CBS-QB3 calculated rates of Sirjean et al. [25] have been adopted for both pathways which are generally in reasonable agreement with the analysis of Tsang et al. [24]. Further resolving and refinement of these unimolecular pathways and reaction rates likely requires calculations utilizing multi-reference methods, as applied in the ring-opening of cyclohexane [26]. Loss of an H-atom from cyclopentane to form a cyclopentyl radical is written in the reverse direction using an estimated rate of 1×10^{14} cm^3 mol^{-1} s^{-1} which is common for such termination reactions.

H-atom abstraction reactions from cyclopentane by small radicals such as Ḣ, Ö, and ȮH were taken from previous experimental and theoretical studies [27,28,29]. Rates for the H-atom abstractors O_2, HO_2, and CH_3 have not been studied by experimental or computational methods for cyclopentane to the authors' knowledge and are excellent candidates for future work. Currently, H-atom abstraction by molecular oxygen was estimated using a rate rule of the $A = n \cdot 9 \times 10^{13}$ cm^3 mol^{-1} s^{-1} and $E = \Delta H + 2 \cdot \overline{R} \cdot (1000\text{K})$ cal mol^{-1}. For the rate rule, A is the pre-

exponential factor, E is the activation energy, n is the number of equivalent hydrogen atoms available, ΔH is the enthalpy of the reaction, and $\overline{R}$ is the molar gas constant. Abstraction of H-atoms by $H\dot{O}_2$ radicals was assumed to be analogous to abstraction from secondary alkyl sites as calculated by Aguilera-Iparraguirre et al. [30] multiplied by the number of equivalent hydrogen atoms available. The rate for abstraction by $H\dot{O}_2$ radicals was further increased by a factor of 1.5 to maintain consistency with the current LLNL alkyl rate rule. In this work, H-atom abstraction by methyl radicals was assumed to be analogous to secondary alkyl abstractions and the current LLNL rate rule was applied accounting for available equivalent hydrogen atoms.

Calculations by Al Rashidi et al. [4] were used for the unimolecular decompositions of the cyclopentyl radical and modified based on comparisons to the more recent experimental measurements and high pressure limit calculations of Manion and Awan [31]. Loss of H-atom from cyclopentyl was increased by a factor of 1.08, while the ring opening to the penten-5-yl radical was increased by a factor of 2.51. The cyclopentyl ring opening rate adopted in this work is very close to the logarithmic average rate between the two studies and within reasonable agreement given their uncertainties. Additionally, increasing the ring opening provides much better agreement between simulations and measurements of the species selectivities in a shock tube by Manion and Awan [31] and of species concentrations in a jet-stirred reactor [1].

Low temperature pathways resulting from the interaction of cyclopentyl radicals and molecular oxygen were largely taken from the work Al Rashidi et al. [4] after removing the local optimizations, or "tunings" because the tunings were not needed in the present kinetic model to obtain good agreement with the experimental validation data. Calculations by Al Rashidi et al. [4] where typically fit to cover the range of 300~1200 K, however for some negligible pathways the fitted rates progress to unphysical values beyond 1200 K. These negligible pathways were removed in the current work to avoid adverse impacts of unphysical rate constants on the computed results and the performance of the numerical solvers.

3.2 Cyclopentene sub-model

Besides the loss of H-atoms, there are two well-known unimolecular decomposition reactions of cyclopentene, which is a major intermediate in the oxidation and pyrolysis of cyclopentane. The first unimolecular reaction is the dehydrogenation to cyclopentadiene and molecular hydrogen, and the current work uses the rate from Lewis et al. [32]. Manion and Awan [31] also provide the most recent assessment of the cyclopentene dehydrogenation reaction which is in good agreement with the value of Lewis et al. [32]. The other unimolecular reaction is the pericyclic formation of vinyl cyclopropane [33], and the current rate was adopted from Lewis et al. [34]. It should be noted that vinyl cyclopropane can then further undergo rapid unimolecular isomerization to the linear pentadiene isomers, and the corresponding rates in this study were adopted from Wellington et al. [35]. Termination of an H-atom with the alkyl-like cyclopenten-4-yl radical was estimated with a value of 1×10^{14} cm^3 mol^{-1} s^{-1}. For the resonantly stabilized cyclopenten-3-yl, an estimation was made via analogy to the high-pressure limit calculation of Harding et al. [36] for the termination of a hydrogen atom with the allyl radical.

Analogies to the cyclopentane rates discussed in Section 3.1 were applied for H-atom abstractions of cyclopentene by small radicals (O_2, $\dot{H}$, $\dot{O}$, $\dot{O}H$, $H\dot{O}_2$, $\dot{C}H_3$) forming the cyclopenten-4-yl radical. H-atom abstractions by $\dot{H}$, $\dot{O}$, $\dot{O}H$, and $H\dot{O}_2$ leading to the formation of the resonantly stabilized cyclopenten-3-yl were estimated via analogy to literature calculations for other C_3–C_5 resonantly stabilized radicals [37,38,39,40]. For the H-atom abstraction by O_2, the analogous rate rule discussed in Section 3.1 was applied with a corrective multiplicative factor of exp(-2) to the pre-exponential factor to account for resonance. Wang et al. [41] calculated the abstraction from

cyclopentene by methyl radical leading to cyclopentene-3-yl radical and their rate is used in the current work. Abstractions of the vinylic hydrogen from cyclopentene were considered minor pathways and were not included in the current work.

Chemically activated H-atom addition pathways for cyclopentene were adopted from the calculations of Wang et al. [42]. H-atom addition to cyclopentene forming cyclopentyl was discussed in Section 3.1, discussed as the decomposition of cyclopentyl. Reactions involving the addition of Ö, ȮH, $HȮ_2$, and $ĊH_3$ radicals have not been extensively studied for cyclopentene and further studies are warranted.

Unimolecular reactions of the cyclopentenyl radicals were modeled using calculations by Wang et al. [42]. While it is known that allylic radical self-recombination reactions occur [43,44], the self-recombination of cyclopenten-3-yl has not been studied to the authors' knowledge and therefore this pathway was neglected in the current work. Similarly, limited information is available regarding the reactions of cyclopenten-3-yl with molecular oxygen or the hydroxyl radical, and these pathways were neglected. Reactions of cyclopenten-3-yl with atomic oxygen were estimated as irreversible reactions using calculations of Ghildina et al. [45] for the cyclopentadienyl system.

A possibly important reaction in the oxidation of cyclopentene is the reaction of cyclopenten-3-yl and $HȮ_2$ radicals. Two sets of products were considered, stabilization to 3-hydroperoxycyclopentene and the chemically activated formation of cyclopenten-3-oxy and hydroxyl radicals. In this work, the current rates are adopted from the calculations by Goldsmith et al. [46] for the allyl + $HȮ_2$ system. Ring opening of the cyclopentene-3-oxy radical was estimated using the work of Wang et al. [47] and written as a ring closure reaction.

3.3 Cyclopentadiene sub-model

For the unimolecular decomposition of cyclopentadiene, only the loss of an H-atom was considered in this work. The high-pressure limit calculation by Harding et al. [36] was used to write the termination of atomic hydrogen with cyclopentadienyl radical. H-atom abstractions forming cyclopentadienyl by atomic hydrogen and methyl radicals were modeled using the calculations of Robinson and Lindstedt [37] and Wang et al. [41] respectively. Abstractions by O_2, Ö, ȮH, and $HȮ_2$ leading to cyclopentadienyl were estimated using the rate rule described in Section 3.2 or analogous reactions [38,39,40]. Due to the limited number of weak C–H bonds in cyclopentadiene, abstractions from the vinylic sites were considered in this work for their potential importance primarily at high temperature (>1000 K) conditions. Rates for the H-atom abstraction by small radicals (O_2, Ḣ, Ö, ȮH, $HȮ_2$, $ĊH_3$) leading to vinylic cyclopentadienyl radicals were estimated by a combination of rate rules and analogy [48,49,50].

H-atom addition, including stabilization and chemically activated, reactions to cyclopentadiene were included in this work using the calculations of Wang et al. [42]. Ö-atom addition to cyclopentadiene forming 1,3-butadiene and carbon monoxide [51] was included using the rate given by Cavallotti et al. [52] for propene and atomic oxygen going to products. Additions by other small radicals (ȮH, $HȮ_2$) were not included in this work as the authors are unaware of studies related to these reactions.

Decomposition of the resonantly stabilized cyclopentadienyl radical to either 1-vinylpropargyl, or propargyl and acetylene was modeled using the calculations by Da Silva [53]. Several recent computational studies from the Mebel group have been adopted in this work to model the oxidation of cyclopentadienyl radicals by O_2, Ö, and ȮH [54,45,55]. Pathways related to methylcyclopentadienes were adopted from Sharma et al. [56] and Dubnikova et al. [57]. Self-recombination of cyclopentadienyl radicals was modeled using the rates given by Cavallotti et al.

[44]. For the addition of $H\dot{O}_2$ with cyclopentadienyl radicals, the analogous rates for stabilization and chemically activated products from Goldsmith et al. [46] were used. The $H\dot{O}_2$ radical addition rates were increased by a factor of 2.5 for the number of equivalent resonant sites, and further increased by a factor of two as a local optimization. Unimolecular reactions of the cyclopentadien-5-oxy radical were modeled using the barrier heights from the potential energy surface calculated by Ghildina et al. [45] and pre-exponential factors were estimated.

3.4 Dimethyl ether sub-model

The dimethyl ether sub-model was developed based on the recent study of ethanol and dimethyl ether binary blends by Zhang et al. [58]. Zhang et al. modified the carbonyl hydroperoxide decomposition rate to 2.5×10^{16} s^{-1} with an activation energy of 43 kcal mol^{-1} to achieve better modeling agreement with their experiments of ethanol/DME mixtures. This modification was adopted in the current kinetic model.

4. Results and discussion

An important feature of any kinetic model is the ability to reproduce the heat release measured experimentally. The heat release manifests itself as a pressure increase in the reacting fuel-air mixture relative to the non-reacting pressure history. Therefore, representative pressure histories from the current RCM experiments and simulations of cyclopentane and dimethyl ether blends were examined and compared to corresponding non-reactive pressure histories. Comparisons for 20 and 40 bar are shown in Fig. 1.

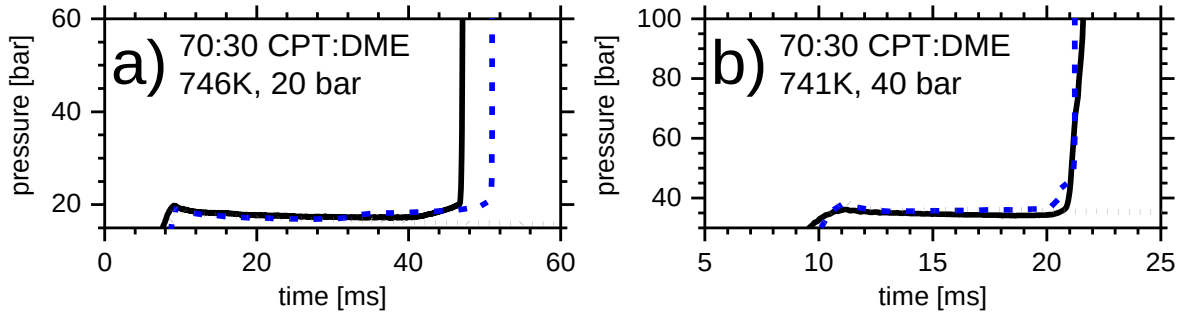

Figure 1. Representative experimental (solid lines) pressure histories of cyclopentane and dimethyl ether binary blends in the NUIG RCM for stoichiometric mixtures of 70:30-CPT:DME. Two simulation results, non-reactive (dotted lines) and reactive (dashed lines) cases, are shown using the current kinetic model. The end-of-compression time is nominally 11 ms.

In Fig. 1, it is interesting to note the lack of significant heat release measured in the 70:30 CPT:DME experiments prior to ignition despite the strong non-Arrhenius or even negative temperature coefficient (NTC) behavior in Fig. 2. For most alkanes, non-Arrhenius plots of ignition delay times are indicators of low temperature chemistry which typically manifests as two-stage ignition. However, in this work there was very little measured or predicted low temperature heat release for mixtures with high concentrations of cyclopentane at all pressures and equivalence ratios considered. This result suggests that cyclopentane suppresses low-temperature heat release. For fuel-lean equivalence ratios with high concentrations of dimethyl ether, two-stage ignition was measured with greater frequency and measurable low temperature release was observed and predicted. The simulated pressure histories are typically in acceptable agreement with the experimental measurements, indicating the heat release is adequately captured in the current model.

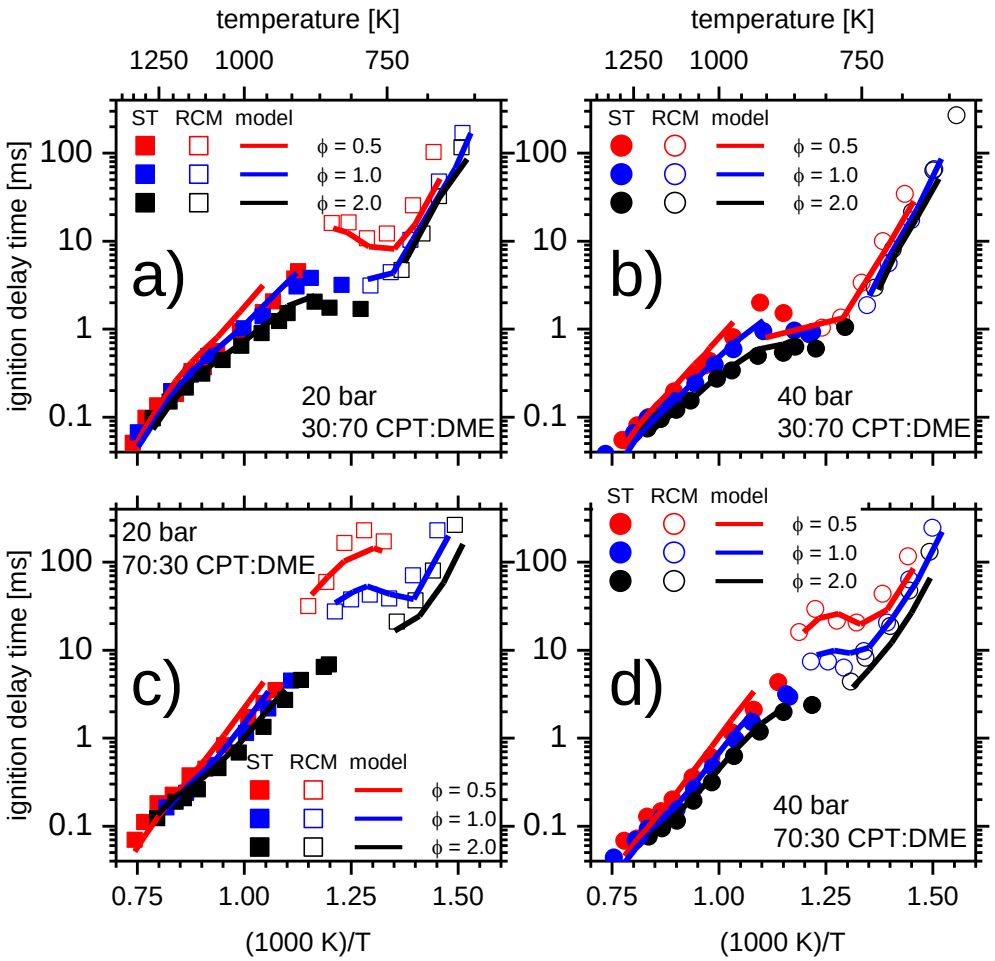

Figure 2. Overall ignition delay time measurements of cyclopentane and dimethyl ether binary blends from the NUIG HPST and RCM in this work. Lines show simulations using the current kinetic model for cyclopentane and dimethyl ether.

Because of the unusual behavior of mixtures with high concentrations of cyclopentane, the reactions controlling the low temperature heat release were investigated. Low temperature exothermicity in the high cyclopentane concentration simulations is primarily derived from oxygen addition to the cyclopentyl radical (~22% of exothermicity), analogous to the important low temperature heat release reactions in alkyl mixtures. Additional but less significant exothermic contributions stem from H-atom abstraction (CPT+ȮH=cyĊ$_5$H$_9$+H$_2$O and HȮ$_2$+HȮ$_2$=H$_2$O$_2$+O$_2$) reactions among others. Competitive endothermic reactions include the concerted elimination of HȮ$_2$ from the cyclopentylperoxy radical (~20% of endothermicity). RO–OH bond breaking of hydroperoxycyclopentene and carbonyl hydroperoxide together account for less than 18% of the modeled endothermicity. In this study, the concerted elimination of HȮ$_2$ is important for both its endothermicity and as a primary source of HȮ$_2$ radicals. At low and intermediate temperature conditions the large quantity of HȮ$_2$ radicals generated from the concerted elimination contributes to H-atom abstractions from fuel components increasing reactivity. Additionally, the oxidation of resonantly stabilized cyclic intermediates such as cyclopenten-3-yl and cyclopentadienyl proceed through stabilized adducts formed from reactions with HȮ$_2$ radicals. These adducts eventually undergo RO–OH bond breaking and subsequent ring opening which enhance the reactivity. At high temperatures, resonantly stabilized radicals consume HȮ$_2$ radicals through chemically activated paths producing reactive hydroxyl radicals and allyloxy radicals.

In the simulations, high dimethyl ether mixtures exhibit their low temperature heat release through familiar paths of molecular oxygen addition to fuel radicals ($CH_3O\dot{C}H_2$ or $cy\dot{C}_5H_9$) and H-atom abstraction from fuel components by hydroxyl radicals. Reactions which are significantly endothermic during ignition simulations include the decomposition of carbonyl hydroperoxide and isomerization of the DME peroxyl radical to ȮOOH. Due to the relatively high concentration of DME in the 30:70 CPT:DME mixtures, the role of cyclopentane related pathways are diminished.

The complete set of ignition delay times measured and simulated in the HPST and RCM from this work are presented in Figure 2. It should be noted that the current simulations of the HPST data do not consider non-ideal effects which are typically important in capturing shock tube ignition delay times longer than ~1 ms. In general, the simulated ignition delay times agree well with the measured ones with a maximum difference of a factor of two. Examining the broader trends of ignition delay times for the binary CPT:DME mixtures, mixtures high in dimethyl ether are more reactive with shorter ignition delay times as expected. Elevated pressures lead to enhanced reactivity for all mixtures and temperatures. At low temperature conditions, ignition delay times for lean mixtures were significantly delayed. This trend can be understood by noting that the mixture stoichiometry was controlled by keeping the nominal oxygen concentration constant while varying the fuel concentration. Therefore, for leaner mixtures the amount of reactive DME was reduced in both binary blends at lean equivalence ratios limiting the amount of the low temperature chemistry through classical pathways.

5. Conclusions

In this work, new experiments in a HPST and RCM measured the ignition delay times of cyclopentane and dimethyl ether blends at engine relevant conditions. The experiments provide valuable insight into the low temperature heat release and ignition timing of binary blends of cyclopentane. An improved kinetic model was developed for cyclopentane, cyclopentene, and cyclopentadiene to properly capture the heat release and ignition delay times in this work. The model can simulate the measurements of this work well, despite the identification of reaction pathways which would benefit from future targeted experimental and theoretical studies.

6. Acknowledgements

Portions of this work were performed under the auspices of the U.S. Department of Energy by Lawrence Livermore National Laboratory under Contract DE-AC52-07NA27344 and were conducted as part of the Co-Optimization of Fuels & Engines (Co-Optima) project sponsored by the DOE Office of Energy Efficiency and Renewable Energy (EERE), Bioenergy Technologies and Vehicle Technologies Offices. The authors from LLNL would also like to thank Dr. Matthew McNenly, Dr. Russell Whitesides, and Dr. Simon Lapointe for access to their computational solvers, tools, and discussion. The authors at NUI Galway recognize funding support from Science Foundation Ireland (SFI) via their Principal Investigator Program through project number 15/IA/3177.

7. References

[1] M.J. Al Rashidi, S. Thion, C. Togbé, G. Dayma, M. Mehl, P. Dagaut, W.J. Pitz, J. Zádor, S.M. Sarathy, Elucidating reactivity regimes in cyclopentane oxidation: Jet stirred reactor experiments, computational chemistry, and kinetic modeling, Proc. Combust. Inst. 36 (2017) 469-477.

[2] M.J. Al Rashidi, J.C. Mármol, C. Banyon, M.B. Sajid, M. Mehl, W.J. Pitz, S. Mohamed, A. Alfazazi, T. Lu, H.J. Curran, A. Farooq, Cyclopentane combustion. Part II. Ignition delay measurements and mechanism validation. Combust. Flame 183 (2017) 372-385.

[3] A. Fridyland, S.S. Goldsborough, M. Al Rashidi, S.M. Sarathy, M. Mehl, W.J. Pitz, Low temperature autoignition of 5-membered ring naphthenes: Effects of substitution, Combust. Flame 200 (2019) 387-404.

[4] M.J. Al Rashidi, M. Mehl, W.J. Pitz, S. Mohamed, S.M. Sarathy, Cyclopentane combustion chemistry. Part I: Mechanism development and computational kinetics. Combust. Flame 183 (2017) 358-371.
[5] S.G. Davis, C.K. Law, Determination of and fuel structure effects on laminar flame speeds of C1 to C8 hydrocarbons, Combust. Sci. Tech. 140 (1998) 427-449.
[6] H. Zhao, J. Wang, X. Cai, Z. Tian, Q. Li, Z. Huang, A comparison of cyclopentane and cyclohexane laminar flame speeds at elevated pressures and temperatures, Fuel 234 (2018) 238-246.
[7] Z. Tian, C. Tang, Y. Zhang, J. Zhang, Z. Huang, Shock tube and kinetic modeling study of cyclopentane and methylcyclopentane, Energy Fuels 29 (2015) 428-441.
[8] B. Sirjean, F. Buda, H. Hakka, P.A. Glaude, R. Fournet, V. Warth, F. Battin-Leclerc, M. Ruiz-Lopez, The autoignition of cyclopentane and cyclohexane in a shock tube, Proc. Combust. Inst. 31 (2007) 277-284.
[9] S.M. Daley, A.M. Berkowitz, M.A. Oehlschlaeger, A shock tube study of cyclopentane and cyclohexane ignition at elevated pressures, Int. J. Chem. Kinet. 40 (2008) 624-634.
[10] V. Simon, Y. Simon, G. Scacchi, F. Baronnet, Experimental and modeling study of the oxidation reactions of n-pentane and cyclopentane, Can. J. Chem. 75 (1997) 575-584.
[11] S. Vranckx, C. Lee, H.K. Chakravarty, R.X. Fernandes, A rapid compression machine study of the low temperature combustion of cyclohexane at elevated pressures, Proc. Combust. Inst. 34 (2013) 377-384.
[12] S.S. Vasu, D.F. Davidson, Z. Hong, R.K. Hanson, Shock tube study of methylcyclohexane ignition over a wide range of pressure and temperature, Energy Fuels 23 (2009) 175-185.
[13] H.J. Curran, W.J. Pitz, C.K. Westbrook, P. Dagaut, J.-C. Boettner, M. Cathonnet, A wide range modeling study of dimethyl ether oxidation, Int. J. Chem. Kinet. 30 (1998) 229-241.
[14] U. Pfahl, K. Fieweger, G. Adomeit, Self-ignition of diesel-relevant hydrocarbon-air mixtures under engine conditions, Proc. Combust. Inst. 26 (1996) 781-789.
[15] G. Mittal, M.P. Raju, C.-J. Sung, CFD modeling of two-stage ignition in a rapid compression machine: Assessment of zero-dimensional approach, Combust. Flame 157 (2010) 1316-1324.
[16] C. Morley, Gaseq, http://www.gaseq.co.uk/
[17] Y. Li, C.-W. Zhou, K.P. Somers, K. Zhang, H.J. Curran, The oxidation of 2-butene: A high pressure ignition delay, kinetic modeling study and reactivity comparison with iso-butene and 1-butene, Proc. Combust. Inst. 36 (2017) 403-411.
[18] G. Kukkadapu, D. Kang, S.W. Wagnon, K. Zhang, M. Mehl, M. Monge-Palacios, H. Wang, S.S. Goldsborough, C.K. Westbrook, W.J. Pitz, Kinetic modeling study of surrogate components for gasoline, jet and diesel fuels: C7-C11 methylated aromatics, Proc. Combust. Inst. 37 (2019).
[19] E.R. Ritter, J.W. Bozzelli, THERM: Thermodynamic property estimation for gas phase radicals and molecules, Int. J. Chem. Kinet. 23 (1991) 767-778.
[20] S. Dooley, M. Uddi, S.H. Won, F.L. Dryer, Y. Ju, Methyl butanoate inhibition of n-heptane diffusion flames through an evaluation of transport and chemical kinetics, Combust. Flame 159 (2012) 1371-1384.
[21] R. Bosque, J. Sales, Polarizabilities of solvents from the chemical composition, J. Chem. Inf. Comput. Sci. 42 (2002) 1154-1163.
[22] M.J. McNenly, R.A. Whitesides, D.L. Flowers, Faster solvers for large kinetic mechanisms using adaptive preconditioners, Proc. Combust. Inst. 35 (2015) 581-587.
[23] ANSYS Chemkin-Pro, Release 19.0
[24] W. Tsang, Thermal decomposition of cyclopentane and related compounds, Int. J. Chem. Kinet. 10 (1978) 599-617.
[25] B. Sirjean, P.A. Glaude, M.F. Ruiz-Lopez, R. Fournet, Detailed kinetic study of the ring opening of cycloalkanes by CBS-QB3 calculations, J. Phys. Chem. A 110 (2006) 12693-12704.
[26] J.H. Kiefer, K.S. Gupte, L.B. Harding, S.J. Klippenstein, Shock tube and theory investigation of cyclohexane and 1-hexene decomposition, J. Phys. Chem. A 113 (2009) 13570-13583.
[27] H.-H. Carstensen, A.M. Dean, Rate constant rules for the automated generation of gas-phase reaction mechanisms, J. Phys. Chem. A 113 (2009) 367-380.
[28] N. Cohen, K.R. Westberg, Chemical kinetic data sheets for high-temperature reactions. Part II, J. Phys. Chem. Ref. Data 20 (1991) 1211-1311.
[29] R. Sivaramakrishnan, J.V. Michael, Shock tube measurements of high temperature rate constants for OH with cycloalkanes and methylcycloalkanes, Combust. Flame 156 (2009) 1126-1134.
[30] J. Aguilera-Iparraguirre, H.J. Curran, W. Klopper, J.M. Simmie, Accurate benchmark calculation of the reaction barrier height for hydrogen abstraction by the hydroperoxyl radical from methane. Implications for C_nH_{2n+2} where n = 2-4, J. Phys. Chem. A 112 (2008) 7047-7054.

[31] J.A. Manion, I.A. Awan, A shock tube study of H atom addition to cyclopentene, Int. J. Chem. Kinet. 50 (2018) 225-242.
[32] D.K. Lewis, J. Bergmann, R. Manjoney, R. Paddock, B.L. Kalra, Rates of reactions of cyclopropane, cyclobutene, cyclopentene, and cyclohexene in the presence of boron trichloride, J. Phys. Chem. 88 (1984) 4112-4116.
[33] J.E. Baldwin, Thermal rearrangements of vinylcyclopropanes to cyclopentenes, Chem. Rev. 103 (2003) 1197-1212.
[34] D.K. Lewis, D.J. Charney, B.L. Kalra, A.-M. Plate, M.H. Woodard, S.J. Cianciosi, J.E. Baldwin, Kinetics of the thermal isomerizations of gaseous vinylcyclopropane and vinylcyclobutane, J. Phys. Chem. A 101 (1997) 4097-4102.
[35] C.A. Wellington, The thermal isomerization of vinylcyclopropane, J. Phys. Chem. 66 (1962) 1671-1674.
[36] L.B. Harding, S.J. Klippenstein, Y. Georgievskii, On the combination reactions of hydrogen atoms with resonance-stabilized hydrocarbon radicals, J. Phys. Chem. A 111 (2007) 3789-3801.
[37] R.K. Robinson, R.P. Lindstedt, On the chemical kinetics of cyclopentadiene oxidation, Combust. Flame 158 (2011) 666-686.
[38] F. Leonori, N. Balucani, V. Nevrly, A. Bergeat, S. Falcinelli, G. Vanuzzo, P. Casavecchia, C. Cavallotti, Experimental and theoretical studies on the dynamics of the $O(^3P)$ + propene reaction: Primary products, branching ratios, and role of intersystem crossing, J. Phys. Chem. C 119 (2015) 14632-14652.
[39] S.S. Vasu, L.K. Huynh, D.F. Davidson, R.K. Hanson, D.M. Golden, Reactions of OH with butene isomers: Measurements of the overall rates and a theoretical study, J. Phys. Chem. A 115 (2011) 2549-2556.
[40] J. Zador, S.J. Klippenstein, J.A. Miller, Pressure-dependent OH yields in alkene + HO_2 reactions: A theoretical study, J. Phys. Chem. A 115 (2011) 10218-10225.
[41] K. Wang, S.M. Villano, A.M. Dean, Reactions of allylic radicals that impact molecular weight growth kinetics, Phys. Chem. Chem. Phys. 17 (2015) 6255-6273.
[42] K. Wang, S.M. Villano, A.M. Dean, Fundamentally-based kinetic model for propene pyrolysis, Combust. Flame 162 (2015) 4456-4470.
[43] P.T. Lynch, C.J. Annesley, C.J. Aul, X. Yang, R.S. Tranter, Recombination of allyl radicals in the high temperature fall-off regime, J. Phys. Chem. A 117 (2013) 4750-4761.
[44] C. Cavallotti, D. Polino, On the kinetics of the C5H5 + C5H5 reaction, Proc. Combust. Inst. 34 (2013) 557-564.
[45] A.R. Ghildina, A.D. Oleinikov, V.N. Azyazov, A.M. Mebel, Reaction mechanism, rate constants, and product yields for unimolecular and H-assisted decomposition of 2,4-cyclopentadienone and oxidation of cyclopentadienyl with atomic oxygen, Combust. Flame, 183 (2017) 181-193.
[46] C.F. Goldsmith, S.J. Klippenstein, W.H. Green, Theoretical rate coefficients for allyl + HO_2 and allyloxy decomposition, Proc. Combust. Inst. 33 (2011) 273-282.
[47] K. Wang, S.M. Villano, A.M. Dean, Ab initio study of the influence of resonance stabilization on intramolecular ring closure reactions of hydrocarbon radicals, Phys. Chem. Chem. Phys 18 (2016) 8437-8452.
[48] K. Mahmud, P. Marshall, A. Fontijn, A high-temperature photochemistry kinetics study of the reaction of $O(^3P)$ atoms with ethylene from 290 to 1510 K, J. Phys. Chem. 91 (1987) 1568-1573.
[49] J.P. Senosiain, S.J. Klippenstein, J.A. Miller, Reaction of ethylene with hydroxyl radicals: A theoretical study, J. Phys. Chem. A 110 (2006) 6960-6970.
[50] J.A. Miller, S.J. Klippenstein, Dissociation of propyl radicals and other reactions on a C_3H_7 potential, J. Phys. Chem. A 117 (2013) 2718-2727.
[51] K. Nakamura, S. Koda, Reaction of atomic oxygen with cyclopentadiene, Int. J. Chem. Kinet. 9 (1977) 67-81.
[52] C. Cavallotti, F. Leonori, N. Baluncani, V. Nevrly, A. Bergeat, S. Falcinelli, G. Vanuzzo, P. Casavecchia, Relevance of the channel leading to formaldehyde + triplet ethylidene in the $O(^3P)$ + propene reaction under combustion conditions, J. Phys. Chem. Lett. 5 (2014) 4213-4218.
[53] G. da Silva, Mystery of 1-vinylpropargyl formation from acetylene addition to the propargyl radical: An open-and-shut case, J. Phys. Chem. A 121 (2017) 2086-2095.
[54] A.D. Oleinikov, V.N. Azyazov, A.M. Mebel, Oxidation of cyclopentadienyl radical with molecular oxygen: A theoretical study, Combust. Flame 191 (2018) 309-319.
[55] G.R. Galimova, V.N. Azyazov, A.M. Mebel, Reaction mechanism, rate constants, and product yields for the oxidation of cyclopentadienyl and embedded five-member ring radicals with hydroxyl.
[56] S. Sharma, W.H. Green, Computed rate coefficients and product yields for c-C_5H_5 + CH_3 → products, J. Phys. Chem. A 113 (2009) 8871-8882.
[57] F. Dubnikova, A. Lifshitz, Ring expansion in methylcyclopentadiene radicals. Quantum chemical and kinetics calculations, J. Phys. Chem. A 106 (2002) 8173-8183.
[58] Y. Zhang, H. El-Merhubi, B. Lefort, L. Le Moyne, H.J. Curran, A. Keromnes, Probing the low-temperature chemistry of ethanol via the addition of dimethyl ether, Combust. Flame 190 (2018) 74-86.